

Forces, torques, and motion everywhere in an ultrasonic standing wave field

D.W. Greve

Department of Electrical and Computer
Engineering, Carnegie Mellon U., Pittsburgh,
PA, USA
DWGreve Consulting, Sedona, AZ, USA
dg07@andrew.cmu.edu

Abstract— Ultrasonic standing waves are used to align and manipulate non-spherical objects. In a previous report, simulations were performed to determine the forces and torques on rod-shaped objects located in stable positions at a standing wave node. Here I determine the forces and torques at all positions in the standing wave field. I present simple expressions with two adjustable parameters that fit these forces and torques. I then use the force and torque expressions to predict the trajectories of objects as a function of time.

Keywords—forces, torques, standing waves, alignment

I. INTRODUCTION

Ultrasonic standing waves have been used to align non-spherical objects for the deposition of ordered two-phase materials [1,2]. This paper addresses the dynamics of the alignment process and simulates the motion of these objects in a standing wave field. This paper expands on previous work where the forces and torques were calculated for objects located at a stable position in a standing wave field [3].

Forces on spherical objects in a standing wave field can be calculated analytically. A qualitative understanding of forces and torques on non-spherical objects can be obtained by considering the net forces on an assembly of spheres approximating the volume of the object [1, 4]. However, quantitative calculation of the forces and torques on non-spherical objects requires a numerical approach [5,6,7].

In this paper, I first calculate the forces and torques on objects as a function of position in a standing wave field using finite element simulation. I then show that the dependence of forces and torques on position can be fit by simple expressions. Finally, I use these expressions to perform a separate finite element simulation to calculate the trajectories of the objects. These calculations give insight into the experimentally observed motions.

II. CALCULATION OF FORCES AND TORQUES

I consider an ultrasonic standing wave field created in a water domain. A 2 MHz acoustic standing wave was created by applying a sinusoidal pressure boundary condition on the bottom surface and a zero acceleration boundary condition on the top surface. The pressure magnitude was 2×10^5 Pa, approximately the pressure produced by a lead-zinc-titanate transducer ideally coupled to the bottom surface and excited by a 40 Vpp sinusoid. The geometry for these simulations is shown in Figure 1. Here $z = 0$ corresponds to an antinode of the

ultrasonic standing wave and a positive rotation θ corresponds to the y axis rotating into the z axis around the x axis.

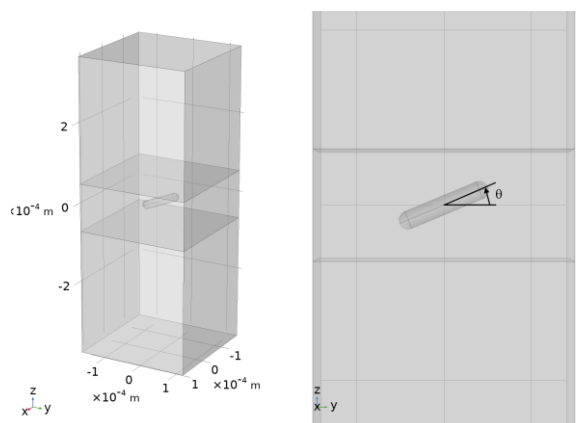


Figure 1. Simulation domain for evaluation of forces and torques: (left) entire simulation domain and (right) detail showing definition of the angle θ (x pointing out of the page).

Rod-shaped fused silica objects with rounded ends were placed at various locations in this standing-wave field. A multiphysics calculation was performed using the pressure acoustics (acpr) and solid mechanics (solid) modules of COMSOL 5.4. The two modules were coupled by requiring that the pressure and the acceleration be continuous at the object boundaries. This calculation yields the fluid velocity and pressure everywhere in the water domain.

Time-averaged torques and forces were calculated using the stress tensor [5,6,7] evaluated from the simulated fluid velocity and pressure. For the geometry considered here, the only force component is in the z direction and the only torque is in the x direction. This is the same approach used in a previous report [3]. Figure 2 shows the simulated force on a 10 μm diameter rod 95 μm in length with rounded ends. The z position is relative to an antinode in the ultrasonic standing wave. The simulated force (circles) can be fit well by a sinusoidal dependence on position with a prefactor that is weakly dependent on the rotation angle (lines). The inset shows that the prefactor for the sinusoidal dependence on z can be fit with a second sinusoidal function of rotation angle. Consequently the force can be written as

$$F_z(z, \theta) = \sin(4\pi z / \lambda) \cdot (A \cos(2\theta) + B) \quad (1)$$

where λ is the acoustic wavelength. The torque (not shown) can be fit by a similar form

$$N_x(z, \theta) = \sin(2\theta) \cdot (C \cos(4\pi z / \lambda) - D) \quad (2)$$

Note that the signs are such that objects have a stable equilibrium point at nodes and an unstable equilibrium at antinodes. An object located at a node tends to align with long side parallel to the nodal plane.

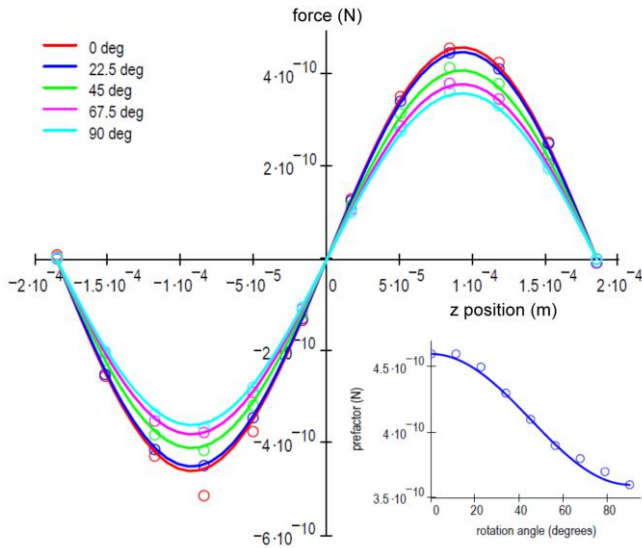


Figure 2. Fit of the force on an elongated object of 10 μm diameter and 95 μm length: (points) force from simulation; (lines) sinusoidal fit to the simulated force and (inset) amplitude of the sinusoid as a function of rotation angle.

Table I shows the fit parameters for fused silica objects of four different geometries. Note that $C > D$, so the torque changes sign between nodes and antinodes. This will lead to complex motions for objects originally located near an antinode. These parameters are for a pressure amplitude of 2×10^5 Pa but scale according to the square of the pressure.

TABLE I. FIT PARAMETERS FOR TORQUE AND FORCE EXPRESSIONS

diam \times length (μm)	A (N)	B (N)	C (N·m)	D (N·m)
10 \times 45	1.5×10^{-11}	1.95×10^{-10}	1.37×10^{-15}	1.1×10^{-15}
10 \times 95	5×10^{-11}	4.1×10^{-10}	5.6×10^{-15}	2.6×10^{-15}
20 \times 45	5×10^{-11}	9×10^{-10}	5.7×10^{-15}	4.1×10^{-15}
20 \times 105	2×10^{-10}	17.5×10^{-10}	2.5×10^{-14}	1×10^{-14}

III. MOTION IN A STANDING WAVE FIELD

I will now use these fits for the torque and force to simulate the motion of objects in a standing wave field. This simulation will be performed using the solid mechanics (solid) and laminar flow (spf) modules of COMSOL 5.4. The geometry of the simulation is shown in Figure 3. The simulation domain is

$100 \times 200 \times 300 \mu\text{m}$ in size (x, y, z) and symmetry at the $x = +100 \mu\text{m}$ plane has been used to reduce the computational effort. The liquid is water and all boundaries other than the symmetry plane have the open boundary condition (zero normal stress). The forces and torques are included by imposing forces at the center of mass and two ends of the object, using the fits described above. The z dependence in equations (1) and (2) corresponds to a pressure node at $z = 0$ and an antinode at $z = +185 \mu\text{m}$. In the following, I report simulations of the object motion for different initial displacements and rotations.

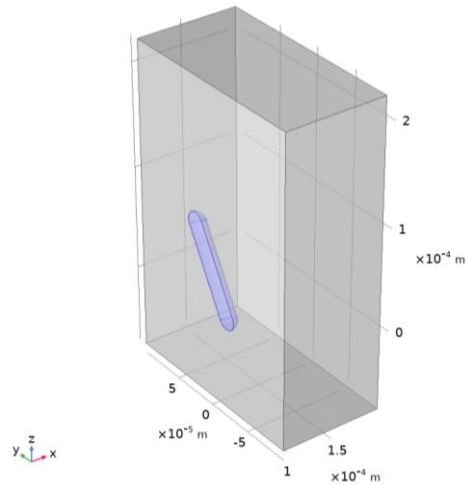


Figure 3. Geometry for simulation of object motion.

Figure 4 shows the rotation θ as a function of time for an object 20 μm in diameter and 105 μm long located at a node. The equilibrium position is reached with minimal overshoot in less than 0.03 sec for all three initial angles.

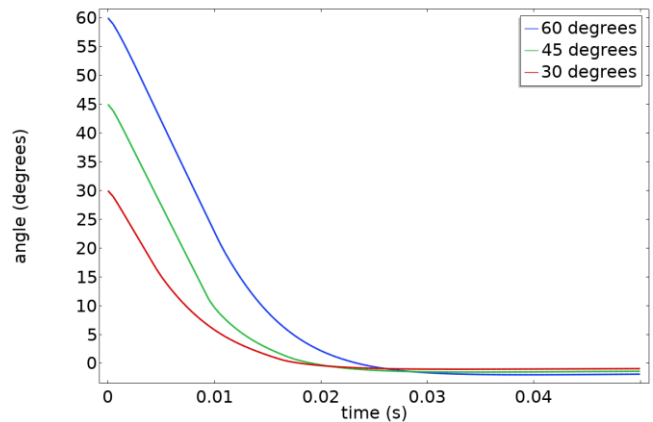


Figure 4. Rotation angle θ as a function of time for a fused silica object 20 μm in diameter and 105 μm long initially located at a node.

Figure 5 shows the center of mass position as a function of time for an object 20 μm in diameter and 105 μm long initially displaced from the node with an initial rotation angle of zero. In all cases there is a moderate amount of overshoot as the object approaches the equilibrium position. Longer simulations (not shown) show the direction of movement reversing and

approaching the nodal position. The overshoot is attributed to a net force on the rod from the fluid motion, as the fluid velocity remains negative after the object crosses the nodal plane. As in the case of the rotational alignment, moderate pressure amplitudes can cause alignment that appears rapid by visual observation, consistent with experiments.

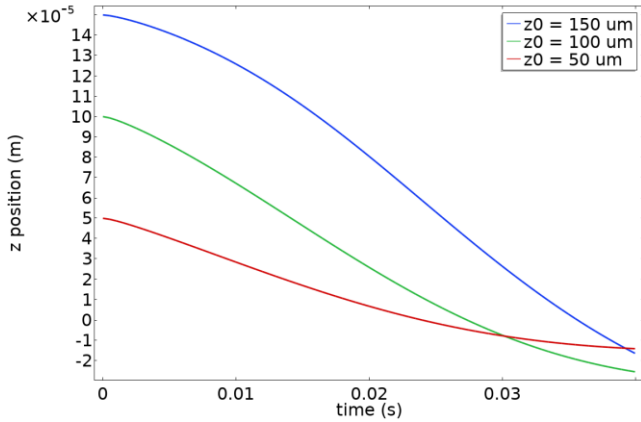


Figure 5. Center of mass position as a function of time for a fused silica object 20 μm in diameter and 105 μm long with an initial rotation angle of zero.

Motion of an object away from a node and with an initial rotation can be complex. This is especially true if the starting point is near an antinode as the torque reverses sign as the object is driven toward a node.

I consider a rod 10 μm diameter, 105 μm in length with initial rotation of 45 degrees. Simulations were performed for four different starting locations ($z(0) = 100, 125, 150,$ and $175 \mu\text{m}$). The largest value of z corresponds to a location close to but just below an antinode. In all cases the center of mass moves toward the node (not shown). The simulated angle as a function of time is plotted in Figure 6. For the two largest values of $z(0)$ the rotation angle initially increases, consistent with the reversal of sign of the torque near the antinode.

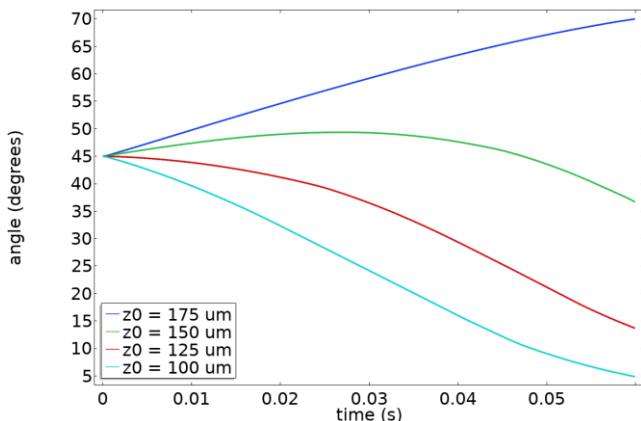


Figure 6. Simulated rotation angle as a function of time for a fused silica object 10 μm diameter and 95 μm length with an initial rotation angle of 45 degrees. When the object is initially close to an antinode the angle initially increases.

Figure 7 shows trajectories of a 10 μm diameter, 95 μm length object for two different starting points. The path followed by the endpoints is shown as a solid black line. The color corresponds to the square of the pressure magnitude so blue indicates a pressure node and red a pressure antinode. In both cases the initial rotation is 45 degrees. For a starting location at $z = +125 \mu\text{m}$ the torque is negative at the starting position, so the angle θ decreases as the object is driven toward the node. In contrast, when starting at $+175 \mu\text{m}$ the angle first increases and then begins to decrease.

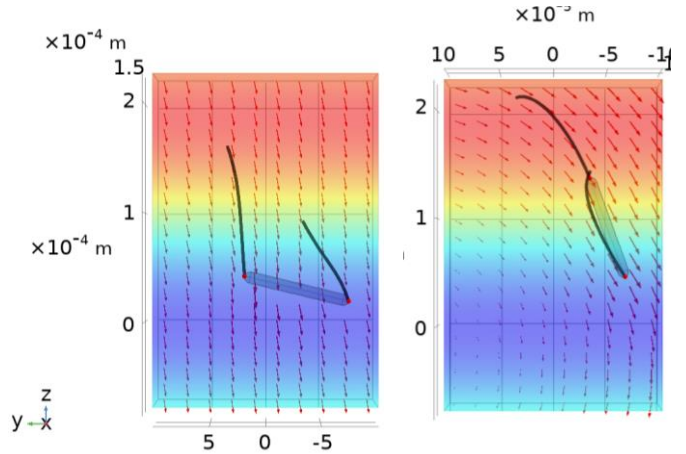


Figure 7. Trajectories of a fused silica object with an initial rotation angle of 45 degrees (left) center of mass starting at $z = 125 \mu\text{m}$ and (right) center of mass starting at $z = 175 \mu\text{m}$. The final position is shown at $t = 0.06 \text{ s}$ (left) and $t = 0.085 \text{ s}$ (right).

Figure 8 and Figure 9 show simulations of objects with the same starting position but with the initial rotation varied. The z position is almost independent of the starting angle although the object is displaced laterally (inset in Figure 9). This effect increases with the rotation angle; there is a reaction force on the object as it imparts motion to the liquid.

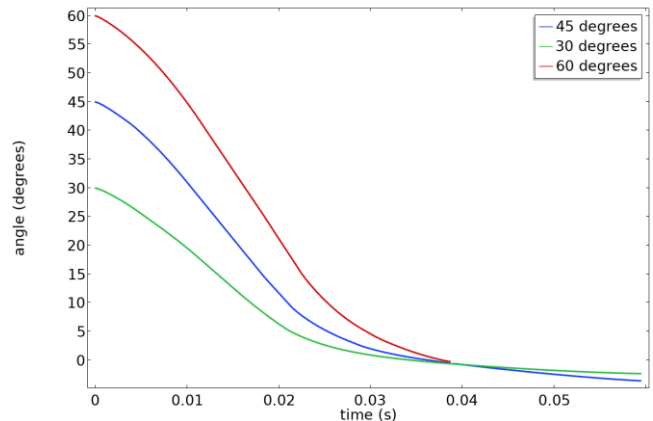


Figure 8. Simulated rotation angle for a 20 μm diameter and 105 μm length object initially located 100 μm from a node with three different initial rotation angles.

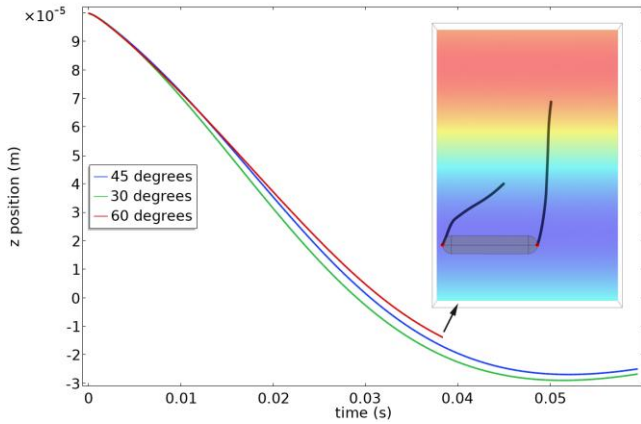


Figure 9. z position for a 20 μm diameter and 105 μm length object initially located 100 μm from a node for three different initial rotation angles.

IV. SUMMARY

Force and torque expressions developed from simulations have been used to predict the motions of rod-like objects in an ultrasonic standing wave. Due to the drag force of the liquid, the time to settle to equilibrium position is larger than predicted in the absence of drag forces. However, standing wave fields of easily attainable magnitude drive the objects to equilibrium on a time scale that appears rapid by visual observation.

V. APPENDIX

Given expressions for the force and torque, it is easy to calculate motions in the absence of fluid damping. For example, for rotational motion of an object located at a node, we have Newton's second law for rotation

$$N = -(C - D) \cdot \sin(2\theta) = I\ddot{\theta} \quad (3)$$

where N is the torque and I is the moment of inertia of the object. This is of the form of the second-order autonomous equation, which appears in many contexts including electrical double layers in liquids and large-amplitude pendulums. Using a trick $d\omega/dt = (d\omega/d\theta) \cdot (d\theta/dt) = \omega \cdot (d\omega/d\theta)$ where ω is the rotational velocity equation (3) can be integrated once to find

$$\omega(\theta) = \pm \sqrt{\frac{C - D}{2I} \cdot (\cos(2\theta_0) - \cos(2\theta))} \quad (4)$$

where θ_0 is the starting angle. This equation can be integrated a second time to get an expression for the time t_1 when the rotational angle first reaches zero, that is

$$t_1 = -\int_{\theta_0}^0 \frac{d\theta}{\sqrt{\frac{C - D}{I} \cdot (\cos(2\theta) - \cos(2\theta_0))}} \quad (5)$$

This expression is useful as a lower limit on the time required for relaxation from an initial rotation. For the object in Figure 4, the predicted t_1 is between 0.002 and 0.0025 sec depending on the initial rotation angle. As expected, this is less than the simulated time that includes the drag due to the fluid.

Newton's second law for the center of mass of an object displaced from a node also has the form $m\ddot{z} = f(z)$ and can be solved in a similar manner.

ACKNOWLEDGEMENTS

I would like to thank I.J. Oppenheim for bringing this interesting problem to my attention.

REFERENCES

- [1] Syojiro Yamahira, Shin-ichi Hatanaka, Mamoru Kuwabara and Shigeo Asai, "Orientation of Fibers in Liquid by Ultrasonic Standing Waves," Jpn. J. Appl. Phys. Part 1 No. 6A, Vol. 39 (2000) pp. 3683–3687.
- [2] R.R. Collino et al., "Deposition of ordered two-phase materials using microfluidic print nozzles with acoustic focusing," Extreme Mechanics Letters 8 (2016) 96–106.
- [3] D.W. Greve, E. Dauson, and I.J. Oppenheim, "Forces and torques on rods in an ultrasonic standing wave," Proceedings of the 2018 International Ultrasonics Symposium.
- [4] Rachel R. Collino, Tyler R. Ray, Rachel C. Fleming, Camille H. Sasaki, Hossein Haj-Hariri, and Matthew R. Begley, "Acoustic field controlled patterning and assembly of anisotropic particles," Extreme Mechanics Letters 5 (2015) 37–46.
- [5] J.H. Lopes, M. Azarpeyvand, and G.T. Silva, "Acoustic interaction forces and torques acting on suspended spheres in an ideal fluid," IEEE Transactions on Ultrasonics, Ferroelectrics, and Frequency Control 63, 186 - 197 (2016).
- [6] Peter Glynne-Jones, Puja P. Mishra, Rosemary J. Boltryk, and Martyn Hill, "Efficient finite element modeling of radiation forces on elastic particles of arbitrary size and geometry," The Journal of the Acoustical Society of America 133, 1885 (2013).
- [7] M.J.H. Jensen and H. Bruus, "First-principle simulation of the acoustic radiation force on microparticles in ultrasonic standing waves," Proceedings of Meetings on Acoustics, Vol. 19, 045001 (2013).